STUDY OF THE EMERGENCE OF SOME HIERARCHIES FROM CERTAIN NUMERICAL PHENOMENA AND OF THEIR IMPLICATIONS

Dan Alexandru IORDACHE[1, 2]

Abstract. *The matter of Hierarchies is especially important for the Complex systems, characterized by a huge number of irreducible uniqueness parameters. Given being the evaluation of the main uniqueness parameters of the complex systems requires the use of computers and this process generates various numerical phenomena [1]-[3], it is expected that some of these numerical phenomena could identify also a certain order among the tremendous number of uniqueness parameters. On the other hand, besides the huge number of specific uniqueness parameters, the complex systems are characterized by some specific co-relations, which generate a restricted number of uniqueness parameters blocks, often considerably more efficient for the complex systems description. As study object, this work has chosen the charge coupled devices (CCDs) – typical representatives of the modern information technology, while the numerical phenomenon preferred to be studied was that of convergence, characterized by the attractor strength.*

Keywords: *Charge Coupled Devices, Dark Current, Numerical phenomena, Attractors strength, Numerical Simulations*

1. Introduction

We studied the dark current of 20 randomly distributed pixels for a backside-illuminated CCD housed in a Spectra Video camera (model SV512V1) manufactured by Pixelvision, Inc. in Beaverton, Oregon. The obtained results referring to the averaged (for each temperature, in the above indicated interval: 222…291 K) dark current and to their standard deviations (for each temperature and pixel) are indicated by **Table 1**.

2. Main Types of Uniqueness Parameters

We will examine the basic case of CCDs operated in a multi-pinned phase (MPP) mode, when the device interface is completely inverted with a high hole concentration, and the surface dark current from the $Si\text{-}SiO_2$ interface will be almost completely suppressed [4]-[7].

a) <u>The elementary basic uniqueness parameters of the CCDs dark current</u> are [8]: (i) the diffusion coefficient D_n, (ii) the effective densities N_v, N_c of the quantum states in the valence and conduction bands, and: (iii) the effective masses m_e, m_h of electrons and holes, respectively, (iv) the concentration N_A of the acceptor impurities,

[1]Prof., Physics Department, University "Politehnica" Bucharest, Romania.
[2]Romanian Scientists Academy, Hon. Member of Section of Information Science and Technology.

(v) the area of a pixel A_{pix}, (vi) the characteristic length x_c of the diffusion process, (vii) the capture cross-sections σ_p, σ_n for holes and electrons, respectively, (viii) the thermal velocity V_{th}, (ix) the intrinsic Fermi energy level E_i, (x) the concentration of traps N_t, (xi) the energy level E_t of the bulk generation-recombination centers,

Table 1

Dark Current and their associated standard deviations (counts/s) in CCDs for 20 randomly selected pixels [8], [9] (obtained by a linear fit to exposure times from 3 s to maximum 100 s)

Coordinates of the pixel	Dark currents/their standard deviations (counts/s) at temperature (K)							
	222	232	242	252	262	271	281	291
41, 120	0.001484 0.003801	0.026228 0.004092	0.100662 0.004996	0.424933 0.005074	1.969514 0.009783	9.228712 0.024020	44.35249 0.116985	217.7895 0.759432
61, 140	0.012969 0.003071	0.040539 0.003757	0.149438 0.005368	0.618415 0.006873	2.505146 0.008665	10.75346 0.028474	48.04459 0.114976	227.3067 0.647973
81, 160	0.008295 0.003253	0.034914 0.003672	0.129242 0.004039	0.526984 0.005315	2.218795 0.011491	9.733896 0.025364	45.19955 0.113001	219.0285 0.725327
101, 180	0.006282 0.002548	0.023767 0.002857	0.095945 0.004635	0.415553 0.005956	1.880534 0.010914	8.843086 0.015512	43.17259 0.132231	214.2660 0.613028
121, 200	0.006063 0.004052	0.029031 0.002548	0.112173 0.005572	0.474378 0.006013	2.053744 0.008049	9.471216 0.023343	44.65022 0.121548	216.9518 0.670435
141, 220	0.008583 0.005063	0.026559 0.003158	0.102486 0.003196	0.440118 0.006127	1.941113 0.011376	9.129981 0.021374	43.64158 0.125649	215.0924 0.668302
161, 240	0.005350 0.003870	0.023663 0.003731	0.093614 0.005877	0.428868 0.004603	1.981857 0.011907	8.892988 0.020439	43.45940 0.130858	215.9305 0.566935
181, 260	0.006074 0.001499	0.022282 0.003255	0.091008 0.003704	0.398030 0.004488	1.838440 0.010817	8.730706 0.23186	42.30294 0.103747	211.0063 0.573907
201, 280	0.017147 0.003917	0.065254 0.003527	0.234979 0.004027	0.868245 0.005721	3.188347 0.014037	12.20961 0.021103	52.23446 0.132068	237.3687 0.691883
221, 300	0.015157 0.002669	0.053210 0.004043	0.189289 0.005228	0.730125 0.006754	2.798395 0.012475	11.44398 0.024583	49.53068 0.132898	229.4021 0.618210
241, 320	0.006311 0.003286	0.033265 0.004260	0.123681 0.005276	0.501478 0.006200	2.086141 0.009312	9.464486 0.026488	44.62626 0.117747	217.6235 0.770354
261, 340	0.012803 0.002676	0.057419 0.004590	0.210351 0.006103	0.818504 0.006205	3.116074 0.012573	12.01514 0.022625	51.54383 0.110135	236.1418 0.698540
281, 360	0.018370 0.004135	0.072716 0.003395	0.253919 0.005953	0.967605 0.007893	3.481746 0.014576	13.30162 0.027987	54.33791 0.117103	242.3072 0.707761
301, 380	0.014709 0.004061	0.060266 0.003328	0.218637 0.004604	0.812199 0.006859	3.061305 0.010382	12.36033 0.026695	53.08315 0.131517	243.6041 0.660860
321, 400	0.003675 0.003399	0.007298 0.002638	0.039933 0.004259	0.244118 0.005207	1.421787 0.009869	7.927352 0.022172	41.07097 0.122311	209.9430 0.644753
341, 420	0.012025 0.004043	0.051089 0.004244	0.196514 0.004187	0.777152 0.005926	2.943100 0.012192	11.37274 0.024829	49.31115 0.091369	231.6490 0.645724
31, 247	0.025084 0.003162	0.084750 0.003970	0.316796 0.005551	1.129892 0.007459	3.855564 0.017382	12.72840 0.029811	51.63198 0.104765	234.6485 0.648644
29, 88	0.009511 0.003712	0.041729 0.004608	0.161847 0.003975	0.647090 0.006759	2.568672 0.013650	10.73541 0.023608	47.82530 0.123029	226.2279 0.683945
188, 471	0.005372 0.003983	0.017136 0.003858	0.074848 0.005254	0.365805 0.006436	1.818186 0.011591	9.043002 0.019539	44.73338 0.136305	223.1231 0.685422
161, 289	0.000314 0.003930	0.002851 0.003629	0.021359 0.004255	0.171535 0.005205	1.154768 0.011748	6.980657 0.023886	37.94227 0.109691	199.2435 0.574439

(xii) the effective masses m_n, m_p of the free electrons and holes, respectively, (xiii) the lower/higher thresholds E_c, E_v of the conduction/valence band, respectively, (xiv) the electrochemical potential μ and the energy gap E_g of the considered semiconductor, respectively (which are also temperature dependent), etc.

In fact, the study of the different complex systems is accomplished – step by step – by means of some alternating results concerning the: a) measured elementary parameters, b) specific co-relations intervening in the description of these systems. It results so a certain “mixture” of the rigorous theoretical considerations and the emerged simplified description by means of some co-relations. This “mixture” leads to some “block” uniqueness parameters, which have to be considered also (see figure).

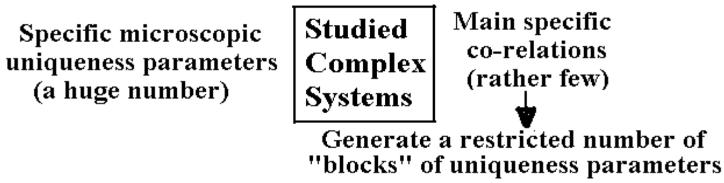

Fig. 1.

The most important intermediary “block” uniqueness parameters, are: (xv) the concentrations *n*, *p*, and, of electrons, holes and of intrinsic carriers, respectively, given by the expressions:

$$n = 2\left(\frac{2\pi \cdot m_n kT}{h^2}\right)^{3/2} \exp\frac{\mu - E_c}{kT}, \quad p = 2\left(\frac{2\pi \cdot m_p kT}{h^2}\right)^{3/2} \exp\frac{E_v - \mu}{kT}, \tag{1}$$

$$n_i = 2\left(\frac{2\pi\sqrt{m_n m_p} \cdot kT}{h^2}\right)^{3/2} \cdot \exp\left(-\frac{E_g}{2kT}\right) = c_n(T) \cdot T^{3/2} \cdot \exp\left(-\frac{E_g}{2kT}\right), \tag{2}$$

(xvi) the net generation-recombination rate U corresponding to the impurities and/or imperfections in the semiconductor lattice, described by the relation:

$$U = \frac{\sigma_p \sigma_n V_{th}\left(n \cdot p - n_i^2\right)N_t}{\sigma_n\left[n + n_i \exp\left(\frac{E_t - E_i}{kT}\right)\right] + \sigma_p\left[n + n_i \exp\left(\frac{E_i - E_t}{kT}\right)\right]}. \tag{3}$$

b) According to the still valid basic theoretical descriptions [4], [5] of the temperature dependence of the diffusion and depletion dark current in CCDs, respectively, the basic co-relations of the studied processes in the examined complex systems (CCDs) are:

$$De^{-}_{diff}(T) = De^{-}_{0,diff} \cdot T^{3} \exp\left(-\frac{E_g}{kT}\right), \tag{4}$$

and (in the approximation of the completely depleted zone: $n,\ p \ll n_i^2$):

$$De^{-}_{dep} = \frac{x_{dep} A_{pix} n_i \left[\sigma_n \exp\left(\frac{E_t - E_i}{kT}\right) + \sigma_p \exp\left(\frac{E_i - E_t}{kT}\right)\right]}{\sigma_p \sigma_v V_{th} N_t} = De^{-}_{0,dep} \cdot T^{3/2} \cdot \exp\left(-\frac{E_g}{2kT}\right) \cdot \sec h\left[\frac{E_t - E_i}{kT} + d\right]. \tag{5}$$

Given being the considered semiconductor (from the CCD composition) is temperature dependent, one finds that the synthesis expression (6) of the dark current in CCDs:

$$De^{-}(T) = De^{-}_{diff}(T) + De^{-}_{dep}(T) = T^{3} \exp\left(\ln De^{-}_{0,diff} - \frac{E_{g,eff.}}{kT}\right) + T^{3/2} \cdot \exp\left(\ln De^{-}_{0,dep} - \frac{E_{g,eff.}}{2kT}\right) \cdot \sec h\left[\frac{E_t - E_i}{kT} + d\right]$$

has to use an effective energy gap $E_{g,eff.}$ (averaged on the corresponding temperatures interval). In fact, the extremely complex composition (involving a tremendous number of different impurities and defects; see Table 2) of the basic semiconductor material of the studied CCD imposes additionally the use of effective parameters.

It results that:

1) the unique elementary uniqueness parameter from the synthesis expression (6) of the basic co-relations expressing the CCD dark current is the effective energy gap $E_{g,eff.}$,

2) the **representative "blocks" of the uniqueness parameters** are:

(i) the diffusion pre-exponential factor, given by the relation:

$$D^{-}_{0,diff} = \frac{D_n A_{pix} c_n^2}{x_c \cdot N_A}, \tag{7}$$

(ii) the depletion pre-exponential factor, given by the expression:

$$De^{-}_{0,dep} = \frac{x_{dep} A_{pix} c_n \sqrt{\sigma_p \sigma_n} \cdot V_{th} N_t}{2}, \tag{8}$$

(iii) the difference $|E_t - E_i|$ between the trap energy E_t and the energy E_i of the intrinsic Fermi level, and:

(iv) "the polarization degree" d of the capture cross-sections for electrons and holes, respectively, defined by the relation:

$$d \equiv pdg_n = \arg\tanh \frac{\sigma_n - \sigma_p}{\sigma_n + \sigma_p} \left[= \frac{1}{2} \ln\left(\frac{\sigma_n}{\sigma_p}\right)\right]. \tag{9}$$

Table 2

Some known values of the traps energy levels,
of both capture cross-sections of free electrons and holes,
respectively, in silicon, as well as of their polarization degree (pdg), implicitly
(see also [10]).

Trap	**Group**	**Energy (eV)**	σ_n **(cm²)**	σ_p **(cm²)**	$k = \sigma_n/\sigma_p$	**pdg**	U **(55°C)** e^-/s
Au_s^-	11	E_i - 0.01	1.4×10^{-16}	7.6×10^{-15}	0.01842	- 1.997	
			5.0×10^{-16}	1.0×10^{-15} $\propto T^{-4}$	0.5	-0.3466	565
MnB	7; 13	E_i - 0.01	9.0×10^{-14}				
$(Mn_i^+ B_s^-)^+$	7; 13	E_i+0.01	2.1×10^{-12}	3.5×10^{-13}	6.0	+ 1.282	
Co_i^+	9	E_i - 0.02	$\sigma = (\sigma_n \cdot \sigma_p)^{1/2} \approx 6.6\times10^{-15}$				3700
Ni_i^+	10						
Pt_i^-	10	E_i+0.02	4.5×10^{-15}	1.09×10^{-14}	2.42	+0.442	970
$CrAl$	6; 13	E_i - 0.048		1.5×10^{-16}			
$CrGa$	6; 13	E_i - 0.058		1.5×10^{-15}			
Zn_s^{--}	12	E_i + 0.07	1.3×10^{-19}	6.6×10^{-15}	1.97×10^{-5}	-5.417	
$MnAl$	7; 13	E_i+0.09	5.0×10^{-15}				
Mn_i^+	7	E_i+0.09			9.4	+1.1204	
$PVp^- \equiv$ *Ecenter*	14	E_i + 0.10	$\sigma = (\sigma_n \cdot \sigma_p)^{1/2} \approx 6.6\times10^{-15}$				70
		E_i + 0.084	3.7×10^{-16}				
VV e^- *trap*	14	E_i + 0.15	4.0×10^{-15}				
Fe_i^+	8	E_i - 0.16	5.0×10^{-14}	7.0×10^{-17}	714.3	+ 3.286	
V_i^{++}	5	E_i - 0.18	5.0×10^{-14}	3.0×10^{-18}	16667	+ 4.86	
Pt_s^+	10	E_i - 0.18		5.4×10^{-14}			
Zn_s^-	12	E_i - 0.21	1.5×10^{-15}	4.4×10^{-15}	0.3409	- 0.538	
Mn_i^{++}	7	E_i - 0.21			23.1 (18.5÷28.3)	+ 1.57	
Mo_i^+	6	E_i - 0.26	1.6×10^{-14}	6.0×10^{-16}	26.67	+ 1.642	
		E_i - 0.223	7.8×10^{-15}	6.0×10^{-16}	13	+ 1.282	
$(Cr_i^+ B_s^-)^-$	6; 13	E_i - 0.26	5.0×10^{-15}	1.0×10^{-14}	0.5	- 0.3466	
PV^+	14	E_i - 0.27					1.8
Ti_i^+	4	E_i+0.27	3.1×10^{-14}	1.4×10^{-15}	22.14	+ 1.549	
Ti_i^{++}	4	E_i - 0.28	1.3×10^{-14}	2.8×10^{-17}	464.3	+ 3.070	
$(Fe_i^+ B_s^-)^+$	8; 13	E_i+0.28 (± 0.02)	1.4×10^{-14} (± 0.02)	1.1×10^{-15} (0.5÷2.5)	13	+ 1.282	
$MnAu$	7; 11	E_i+0.30					
Pt_s^-	10	E_i+0.31	3.4×10^{-15}				
Cr_i^{++}	6	E_i+0.32	2.3×10^{-13}	1.1×10^{-13}	2.091	+ 0.369	
		E_i+0.30	2.0×10^{-14}	4.0×10^{-15}	5	+ 0.805	
VV hole trap	14	E_i - 0.33		2.0×10^{-16}			
$OV^- \equiv$ *A center*	16	E_i+0.37	1.0×10^{-14}				
all *Mn* Traps	7	$\sigma = (\sigma_{min} \cdot \sigma_{max})^{1/2} \approx 1.0\times10^{-15}$; $\cdot\sigma_{max}/\sigma_{min} \sim 10^6$					6400

3. Main Types of Numerical Phenomena met in the Frame of the Uniqueness Parameters Evaluation

For brevity, the main types of numerical phenomena met in the frame of the evaluation of the main uniqueness parameters are presented by Figure 1.

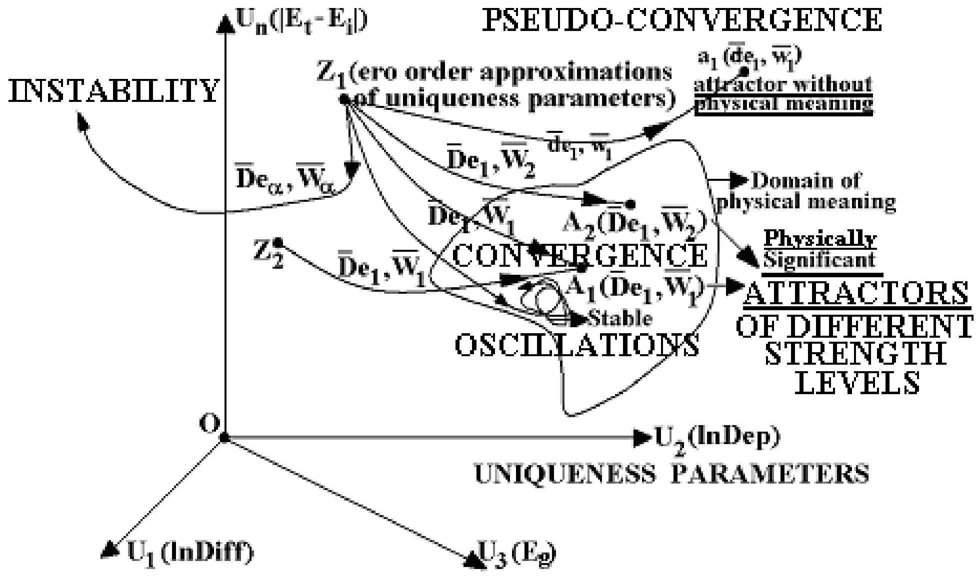

Fig. 1. Main types of numerical phenomena from the uniqueness parameters evaluation.

To be possible to compare the convergence speed corresponding to the main uniqueness parameters, it is necessary to create firstly a certain “basin” of the zero-order approximations, in order to find the consequences of different initial zero-order sites. In this aim, our study started from the: a) modulus $E_{g,Lin}$ of the slope of the line joining the points of extreme temperatures (222 and 291 K, for the experimental data) of the plot $De^{-}(T) = f\left(\frac{1}{kT}\right)$, b) the value $E_{g,Sze}$ of the same parameter indicated by the Sze’s monograph [7]. In following, it is calculated the average of these 2 values: $E_{g,Ave} = \frac{1}{2}\left(E_{g,Sze} + E_{g,Lin}\right)$, and finally the zero-order approximations of the energy gap are introduced by means of the relation: $E_g^{(0)}(m) = E_{g,Ave} + \frac{m}{10}\left(E_{g,Sze} - E_{g,Lin}\right)$, where m is an integer inside the set m = -10; -9; … 0; 1; … 10.

Table 3 presents the obtained results of the accomplished calculations for the zero-order approximations of the energy gap $E_g^{(0)}(m)$, corresponding to 4 chosen pixels and to the above indicated set m = -10; -9; … 0; 1; … 10.

Table 3

Final results concerning the values of the uniqueness parameters $E_g, \ln Diff, \ln Dep$ and $|E_t - E_i|$, obtained by means of the classical gradient method.

Coordinates of the pixel	E_g Zero-order approximation m	$E_{g,eff.}$ (eV)	ln*Diff*	ln*Dep*	$\lvert E_t - E_i \rvert$, meV	Numerical phenomenon & Attractor
61, 140	-10	0.580869*	9.402933*	39.026176*	381.94396*	**Pseudo-convergence**
	-8	0.564653*	8.573753*	40.444841*	414.60294*	
	-6	1.072556	31.079047	17.52459	28.92168	**Very strong attractor**
	-4	1.072556	31.079047	17.52459	28.92168	
	-2	1.072556	31.079047	17.52459	28.92168	
	0	1.072556	31.079047	17.52459	28.92168	
	2	1.072556	31.079047	17.52459	28.92168	
	4	1.072556	31.079047	17.52459	28.92168	
	6; 8 & 10	**Instability** starting from iteration 4 (m = 6) and 2 (m = 8 and 10), respectively				
121, 200	-10	1.067221	30.865956	15.540974	13.31129	**Weak attractor; additionally, medium amplitude oscillations**
	-8	1.067238	30.866604	15.567840	12.93887	
	-6	1.067272	30.867992	15.659601	13.543185	
	-4	1.067263	30.867633	15.630247	13.350595	
	-2	1.067251	30.867136	15.596534	13.128485	
	0	1.067257	30.867372	15.611681	13.22839	
	2	1.067259	30.867458	15.617526	13.2669	
	4; 6; 8; 10	**Instability** starting from iteration 4 (m = 4) and 2 (m = 6; 8 and 10), respectively				
241, 320	-10	1.074871	31.172302	15.917362	11.094875	**Extremely Weak attractor; additionally, large amplitude oscillations**
	-8	1.075900	31.212400	16.033195	9.955040	
	-6	1.075840	31.210004	16.349191	6.748465	
	-4	1.075873	31.211324	16.765059	8.779725	
	-2	1.075894	31.212169	15.976038	9.669870	
	0	1.075681	31.203713	15.338220	6.802035	
	2	1.075685	31.203874	15.336640	6.792465	
	4; 6; 8; 10	**Instability** starting from iteration 3 (m = 4) and 2 (m = 6; 8 and 10), respectively				
31, 247	-10	0.587015*	10.54143*	44.932172*	406.378745*	**Pseudo-convergence**
	-8	**Instability** starting from iteration 9				
	-6	0.574936*	9.935104*	45.115503*	472.32972*	**Pseudo-convergence**
	-4	1.190187*	35.636207	19.734559	9.742655	**Extremely Weak pseudo-attractor; additionally, large amplitude oscillations**
	-2	1.190174*	35.635711	19.830541	10.175875	
	0	1.190169*	35.635528	19.859227	10.302720	
	2	1.190204*	35.636852	19.641657	9.317010	
	4	1.190280*	35.639586	19.217493	7.276885	
	6	1.190267*	35.639176	19.303182	7.692265	
	8; 10	**Instability** starting from iteration 2				

Among the results synthesized by Table 3, the most meaningful are probably those corresponding to the pixel of coordinates 121 and 200 - while for the values of m between –10 and +2: a) not less than the first 5 figures of the uniqueness parameter E_g remain invariant, b) for the uniqueness parameter $\ln Diff$ only the first 4 figures are preserved, c) for the uniqueness parameter $\ln Dep$ only the first 2 figures are constant, while for: d) $|E_t - E_i|$ only the first figure is kept. It results the following hierarchy of these uniqueness parameters: a) E_g (the strongest), b) $\ln Diff$ (the second one, even its strength is very near to E_g, c) $\ln Dep$ (considerably weaker), and: d) $|E_t - E_i|$ (but not too far from $\ln Dep$).

Given being the polarization degree *pdg* was introduced finally, it is to have a strength expected to be considerably weaker than those of the other 4 considered uniqueness parameters.

That is why, we will compare the *pdg* effects on the description accuracy only with the "weakest" previous uniqueness parameter ($|E_t - E_i|$) in order to avoid that its effects be "covered" by other ones much stronger.

The obtained results show that taking into account also the 5th uniqueness parameter *pdg*, and starting from the regression line

$$|\arg\sec h[De - De_{diff} = f(De_{dep(}\sigma_n = \sigma_p)| = F(1/kT)$$

it is possible to obtain rather accurate values of the dark currents for all temperatures corresponding to 17 pixels (from the total of 20), namely accuracy:

a) under 5% for 10 pixels,

b) between 5 and 10% for other 6 pixels, while:

c) for the pixel 321, 400 the accuracy reduces to only 17.47%.

4. Brief examination of the Hierarchies matter in the frame of the numerical game Sudoku

There are some reasons to prefer the numerical game Sudoku relative to other somehow similar games [as the "Game of life" (conceived by John H. Conway [11]) [12], [13], pp. 204-205, e.g], namely:

a) the number of possible different Sudoku (initial) diagrams: approx. 5.4 billions [14] is almost equal to the present number of (living) human beings,

b) the product $P_i = \prod_{j=1}^{n} N_{ji}$ of the virtual populations of the entangled figures inside the different small Sudoku cells is of the same magnitude order (approx. 10^{30}) as the number of bytes flowed in a human body during his average life duration.

The accomplished study pointed out a certain interesting numerical phenomenon intervening in the processing of Sudoku diagram:

(i) the entanglement "clouds" inside a Sudoku diagram are non-uniform,

(ii) the entanglement density irregularities indicate some local priorities of some figures.

In this aim, we ask the readers to look at the next figure 2.

		A			B			C		
		a	b	c	d	e	f	g	h	i
D	1	6	348	1489	1235	234	7	12389	2389	1289
	2	179	5	2	8	36	136	1369	1369	4
	3	148	348	148	236	9	1236	7	5	1268
E	4	2589	268	589	2356	1	2356	4	7	25689
	5	2578	2678	578	9	2367	4	12368	2368	12568
	6	24579	1	3	2567	8	256	269	269	2569
F	7	12478	9	6	1237	5	123	238	2348	278
	8	3	247	47	267	267	8	5	1	2679
	9	12578	278	1578	4	267	12679	2689	2689	3

Fig. 2. Main types of numerical phenomena
from the uniqueness parameters evaluation.

One finds easily the following irregularity: while the figures 4 are present on the line D3 in the square AD, they are missing in the following squares BD and CD. According to the Sudoku rules, the presence of the figure 4 in the line (row) D3 is obligatory, hence the figures 4 from the cells a3 and b3 are dominant in the square AD, and the other figures 4 from this square (those from the cells b1 and c1) can be suppressed!

Conclusions

The identification of the hierarchies present both in certain complex physical systems (as the charge coupled devices, e.g.) or in the frame of some numerical simulations (as the one achieved by means of the Sudoku game) allows:

a) a best choice of the uniqueness parameters, in order to ensure a very good description accuracy by means of a rather reduced number of such parameters,

b) the achievement of the dis-entanglement of some intricate systems, of the Sudoku diagrams, particularly.

R E F E R E N C E S

[1] R. Courant, K. Friedrichs, H. Lewy "On the Partial Difference Equations of Mathematical Physics", *Math. Ann.*, **100**, 32(**1928**).

[2] P. P. Delsanto, D. Iordache, C. Iordache, E. Ruffino "Analysis of the Stability and Convergence in FD Simulations of the 1-D Ultrasonic Wave Propagation", *Mathl. Comp. Modelling (UK),* **25**(6) 19-29(**1997**).

[3] D. Iordache, P. P. Delsanto, M. Scalerandi "Pulse Distortions in the FD Simulations of Elastic Wave Propagation", *Mathl. Comp. Modelling (UK),* **25**(6) 31-43(**1997**).

[4] W. Shockley, W. T. Read "Statistics of the Recombination of Holes and Electrons", *Phys. Rev.*, **87**, 835(**1952**).

[5] R. N. Hall "Electron-Hole Recombination in Germanium", *Phys. Rev.,* **87**, 387(**1952**).

[6] A. S. Grove, Physics and Technology of Semiconductor Devices, J. Wiley, New York, **1967**.

[7] S. M. Sze, Physics of Semiconductor Devices, J. Wiley, New York, 2nd edition, **1981**.

[8] R. Widenhorn, M. M. Blouke, A. Weber, A. Rest, and E. Bodegom, "Temperature dependence of dark current in a CCD", in "Sensors and Camera Systems for Scientific, Industrial, and Digital Photography", *Proc. SPIE*, **4669**, 193-201(**2002**).

[9] R. Widenhorn, E. Bodegom, D. Iordache, I. Tunaru "Computational Approach to Dark Current Spectroscopy in CCDs as Complex Systems. I. Experimental Part and Choice of the Uniqueness Parameters", *Scientific Bulletin of "Politehnica" University Bucharest, Series A: Applied Mathematics and Physics,* **72**(4) 197-208(**2010**).

[10] D. Iordache, P. Sterian, I. Tunaru "Charge Coupled Devices (CCDs) as Particle Detectors", *Hindawi,* http://dx.doi.org/10.1155/**2013**/425746.

[11] M. Gardner, *Scientific American*, **223**(4) 120(1970) … **233**(6) 119(1975).

[12] P. Bak, K. Chen, M. Creutz, *Nature*, **342**, 780(**1989**).

[13] Lui Lam *"Nonlinear Physics for Beginners: Fractals, Chaos, Solitons, Pattern Formation, Cellular Automata and Complex Systems",* World Scientific, 1998.

[14] *** "Dans un Sudoku, y a-t-il un nombre minimal de cases pré remplis?", *Science et Vie* no. 1161, p. 123, Juin **2014**.